



## Article

**Cite this article:** Rana AS, Kunmar P, Mehta M, Kumar V (2023). Glacier retreat, dynamics and bed overdeepenings of Parkachik Glacier, Ladakh Himalaya, India. *Annals of Glaciology* 64(92), 254–267. <https://doi.org/10.1017/aog.2023.50>

Received: 21 July 2022

Revised: 2 June 2023

Accepted: 9 June 2023

First published online: 18 July 2023

**Keywords:**

Glacier changes; ice thickness; Ladakh Himalaya; surface ice velocity; Suru River valley

**Corresponding author:**

Vinit Kumar; Email: [vinitkumark17@gmail.com](mailto:vinitkumark17@gmail.com)

# Glacier retreat, dynamics and bed overdeepenings of Parkachik Glacier, Ladakh Himalaya, India

Ajay Singh Rana<sup>1,2</sup>, Pankaj Kunmar<sup>1,3</sup>, Manish Mehta<sup>1,2</sup> and Vinit Kumar<sup>1,2</sup> 

<sup>1</sup>Wadia Institute of Himalayan Geology, Dehradun, 248001, India; <sup>2</sup>Academy of Scientific and Innovative Research, Ghaziabad, 201002, India and <sup>3</sup>Hemvati Nandan Bahuguna Garhwal University Srinagar, Srinagar, 246174, Uttarakhand, India

**Abstract**

This study describes the morphological and dynamic changes of Parkachik Glacier, Suru River valley, Ladakh Himalaya, India. We used medium-resolution satellite images; CORONA KH-4, Landsat and Sentinel-2A from 1971–2021, and field surveys between 2015 and 2021. In addition, we used the laminar flow-based Himalayan Glacier Thickness Mapper and provide results for recent margin fluctuations, surface ice velocity, ice thickness, and identified glacier-bed overdeepenings. The results revealed that overall the glacier retreated by  $-210.5 \pm 80$  m with an average rate of  $4 \pm 1$  m a<sup>-1</sup> between 1971 and 2021. Whereas a field study suggested that the glacier retreat increased to  $-123 \pm 72$  m at an average rate of  $-20 \pm 12$  m a<sup>-1</sup> between 2015 and 2021. Surface ice velocity was estimated using COSI-Corr on the Landsat data. Surface ice velocity in the lower ablation zone was  $45 \pm 2$  m a<sup>-1</sup> in 1999–2000 and  $32 \pm 1$  m a<sup>-1</sup> in 2020–2021, thus reduced by 28%. Further, the maximum thickness of the glacier is estimated to be  $\sim 441$  m in the accumulation zone, while for glacier tongue it is  $\sim 44$  m. The simulation results suggest that if the glacier continues to retreat at a similar rate, three lakes of different dimensions may form in subglacial overdeepenings.

**1. Introduction**

Considering their sensitivity and as a most direct and apparent visible indicator of regional climate change, Himalayan glaciers have been subjected to numerous studies, from field-based investigations to the modern state-of-the-art remote sensing approach, for more than a century (Bolch and others, 2012; Dobhal and others, 2013; Brun and others, 2017; Schmidt and Nüsser, 2017; Nüsser and Schmidt, 2021).

Since the 1990s, the advancement in remote sensing and in situ-based glacier monitoring results suggested an accelerated glacier melting and mass loss in the Himalaya and surrounding regions (Pratap and others, 2016; Brun and others, 2017) that has caused a substantial modification of glacial hydrology (Akhtar and others, 2008; Nie and others, 2021), river runoff and contributed to the ongoing rising sea level (Zemp and others, 2019; Lee and others, 2021). Accelerated glacier retreat and surface morphological changes due to ongoing climate warming result in the development of new and expansion of the existing glacial lakes (supraglacial and moraine-dammed) that could be a potential source of glacial lake outburst floods in the Himalaya (Schmidt and others, 2020; Shugar and others, 2020; Shukla and Sen, 2021; Kumar and others, 2021a). However, systematic and quantitative monitoring of the glaciers, viz., field and remotely-sensed based changes in a frontal position (Kumar and others, 2017, 2021b; Garg and others, 2018; Mal and others, 2019), mass balance (glaciological and geodetic), debris thickness, and its role in glacier melting (Dobhal and others, 2013; Pratap and others, 2015; Bhushan and others, 2018; Mehta and others, 2021), ice thickness and volume (Gantayat and others, 2014; Mishra and others, 2018; Farinotti and others, 2019), formation and expansion of glacial lakes (Shukla and others, 2018; King and others, 2019), surface ice velocity (Tiwari and others, 2014; Shukla and Garg, 2020), and fluctuation of equilibrium line altitude (Kayastha and Harrison, 2008; Kumar and others, 2021c), has been done in and around the Himalayan region.

Fieldwork in the Himalayan terrain is challenging due to rugged topography and harsh climatic conditions. Based on field approaches, very few studies have been conducted on the same glacier for long-term monitoring to understand the state of the glacier under ongoing climate change (Azam and others, 2016; Dobhal and others, 2021; Mehta and others, 2021, 2023). Inadequate ice thickness and mass balance data make ice volume estimation extremely difficult for the Himalayan glaciers (GlaThiDa Consortium, 2019; Kumari and others, 2021; Mishra and others, 2021). In contrast, understanding the ice thickness and distribution is foremost required for the Himalayan glaciers. However, existing approaches, like remote sensing, cannot directly estimate the glacier thickness. Based on ground penetrating radar, very few studies (only 14 to date) have been carried out on glacier thickness in the Indian Himalaya (Mishra and others, 2022). Therefore, numerous methods and models have been used to estimate the ice thickness distribution and volume of the glaciers in the Himalaya and other regions, e.g. GlaThiDa (Welty and others, 2020), the consensus global glacier thickness models

© The Author(s), 2023. Published by Cambridge University Press on behalf of International Glaciological Society. This is an Open Access article, distributed under the terms of the Creative Commons Attribution licence (<http://creativecommons.org/licenses/by/4.0/>), which permits unrestricted re-use, distribution and reproduction, provided the original article is properly cited.

[cambridge.org/aog](http://cambridge.org/aog)



(Farinotti and others, 2019; Millan and others, 2022), and regional efforts (e.g. Frey and others, 2014). These models are essential without field measurements and can estimate the thickness and volume of a glacier.

In the present study, we used the Himalayan Glacier Thickness Mapper (HIGTHIM) tool, a semi-automated approach based on the laminar flow method (Kulkarni and others, 2019, HIGTHIM manual), utilizing the relation between glacier surface velocity and ice thickness (Cuffey and Paterson, 2010; Gantayat and others, 2014). Further, the HIGTHIM tool is used to estimate the depth, water volume of the potential lakes and identify the glacial bed topography for overdeepening sites. Moreover, field observations (2015–2021) and a feature tracking algorithm in COSI-Corr on Landsat data are used to provide recent changes (snout fluctuations, surface morphology, and surface ice velocity). A model-based approach has been carried out over the Parkachik Glacier for the first time.

## 2. Study area

Parkachik Glacier is one of the largest glacier in the Suru River valley (34°02'N and 76°00'E), covering an area of ~53 km<sup>2</sup> and is ~14 km long and northward trending. The glacier originates from the Nun (7135 m a.s.l.) and Kun (7077 m a.s.l.) peaks south of the Suru River. Parkachik Glacier is a valley glacier with four accumulation basins (thus has four flow units), which all feed through icefalls into a glacier tongue of approximately 7 km long and 800 m wide. Moreover, prominent ogives occur over the entire length of the glacier tongue below the icefalls, which makes the glacier surface undulating and prone to supraglacial lake development (Fig. 1). The Suru River valley is a part of the Southern Zaskar Ranges, western Himalaya. The Suru River valley has 252 glaciers covering 11% of the catchment area, and the average annual snowline altitude of the basin is 5011 ± 54 m a.s.l. (Shukla and others, 2020a). Parkachik Glacier is known by different names, such as 'Ganri Glacier' (Toposheet of 1906, Workman and Workman, 1909) and 'Kangriz Glacier' (Toposheet of 1962, Garg and others, 2018).

Parkachik Glacier terminus is dynamic (calving from the west) and has formed several recessional moraines and mounds in the proglacial area (Garg and others, 2018, 2019; Kumar and others, 2021c). Due to the glacier recession, a proglacial lake was formed after 2015 at ~3600 m a.s.l. on the west part of the terminus and expanded rapidly. Numerous geomorphological (series of lateral, hummocky, and recessional moraines) features are formed in the periphery of the glacier, which suggests that the glacier was very active in the past (2.3 ± 0.2 ka till the present) (Kumar and others, 2021c). These geomorphological features are evidence of glaciation/deglaciation phases observed from the glacier front (~3650 m a.s.l.) to ~2 km downstream near Parkachik village (3550 m a.s.l.).

The mid-latitude westerlies are the important source of moisture supply to the study area, with a wide variability in snowfall during winters (Kumar and others, 2021c). The instrumental meteorological data from the study area is not available. However, without meteorological data, Climate Research Unit Time Series (CRU-TS 4.03) data from 1901–2018 have been used to infer the climatic conditions in the study area (Harris and others, 2020; Mehta and others, 2021). Mehta and others (2021) suggested that the mean monthly minimum temperature (−10°C) in winter (January) and the average minimum monthly precipitation (11 mm) occurred in November. Further, the maximum monthly mean temperature (18°C) and average precipitation (71 mm) were recorded in summer.

## 3. Material and methods

### 3.1. Datasets and pre-processing

In this study, geospatial techniques on multispectral and multi-temporal satellite scenes from CORONA KH-4 (1971), Landsat 7 ETM+ (1999–2000, 2002, and 2009), Operational Land Imager (OLI) (2020–2021), and Sentinel-2A (2021) were used to get the preliminary information of glacier outline and frontal position. Declassified CORONA KH-4 (used for area and length), Landsat and Sentinel-2A imageries (used for area, length, and surface ice velocity), and ASTER (GDEM) were utilized for topographic information, generating contours for input in the HIGTHIM tool (Table 1).

First, the acquired satellite images were co-registered by the projective transformation method using the Landsat ETM+ for the year 1999. However, the CORONA KH-4 image subset was co-registered using a two-step approach (i) Projective transformation using 23 ground control points (GCPs) and (ii) Spline adjustment of the subset image (Bhambri and others, 2012). The road intersection and the rocky mountains, convergence of streams and edges were used as GCPs, which were acquired from Landsat ETM+ 1999 images. We adopted the standard image rectification and interpretation procedure as documented by several workers (Goossens and others, 2006; Bhambri and others, 2012; Chand and Sharma, 2015; Shukla and Ali, 2016; Shukla and Garg, 2019). After that, the glacier outline was delineated using manual digitization on a standard false color composite (incorporating a standard combination of spectral bands; SWIR-NIR-G). The manual delineation of the glacier boundary is labor extensive, but having a high degree of accuracy is still in practice (Garg and others, 2017; Kaushik and others, 2019). Further, the extracted glacier boundary for the year 2021 was used to estimate the ice thickness distribution. Moreover, the length changes of the glacier were quantified using the parallel line method for which collateral strips spaced at an 80 m distance were drawn between the two glacier outlines (Schmidt and Nüsser, 2009). The average distance of these collateral strips was considered to be the total frontal retreat of the Parkachik Glacier. In addition, the glacier boundary and frontal position extracted from the satellite data were validated during the field.

### 3.2. Glacier survey

Fieldwork has been carried out on the Parkachik Glacier since 2015 using a differential global positioning system; changes in frontal position and area have been monitored annually with the help of ground control points taken (stable boulders from right, left, and center) with an accuracy of <1 cm near the glacier front (see Fig. 4). Further, the in situ measurements of glacier surface lowering, debris thickness, and frontal changes were observed from 2015 to 2021. The distance from these reference stations (to the glacier snout) was measured using a measuring tape up to the glacier base from the snout's left, right and center. Average length change was calculated based on the average recession of the glacier from left, right, and center parts for every studied year. The field-based monitoring of the glacier recession and area change was done following the methods given in our recent studies (Kumar and others, 2017; Mehta and others, 2021, 2023). In addition, several features representing higher glacier melting, e.g. supraglacial ponds, ice cliffs, and patchy debris cover (thin and thick), were observed.

### 3.3. Surface ice velocity

The surface ice velocity was calculated using the optical image correlation technique from repeated Landsat images for two consecutive years (1999–2000 and 2020–2021). The method is based

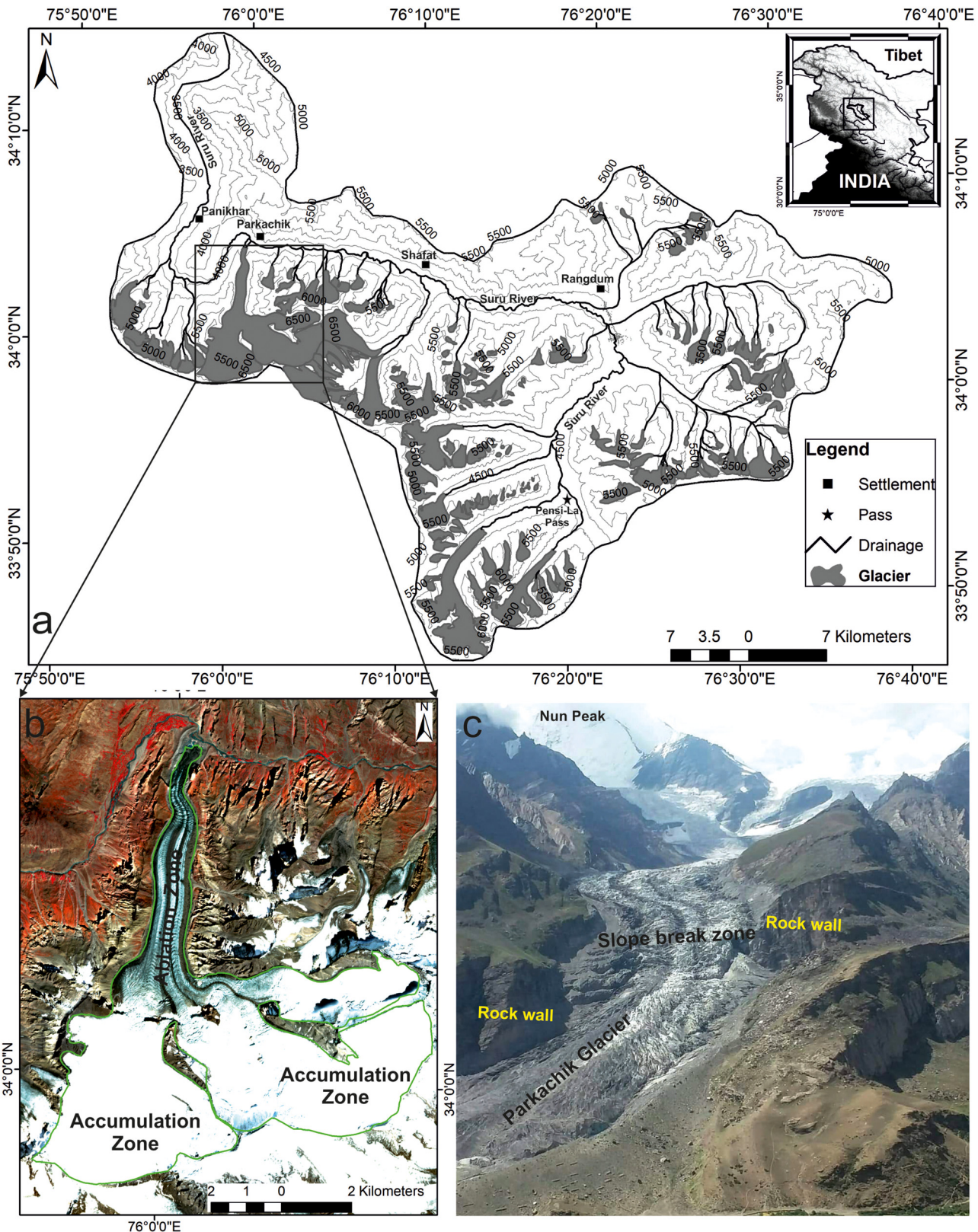


**Figure 1.** (a) Location of the Suru River basin and Parkachik Glacier (inset). (b) Sentinel-2A (2021) image showing the Parkachik Glacier. (c) A Photograph of the glacier showing geological and geomorphic features on and around the glacier. The glacier outlines and drainage are digitized manually from the Sentinel-2A (2021) image and contour line elevation data from ASTER GDEM (2011).

on the Co-registration of Optically Sensed Images and Correlation (COSI-Corr) software, which is a free plug-in module integrated into ENVI that provides tools to accurately orthorectify, co-register, and correlate the remotely sensed images developed by (Leprince and others, 2007), and described in detail by

Scherler and others (2008). COSI-Corr uses a Fourier-based highly advanced matching program that offers sub-pixel accuracy and is widely used to measure glacier movements (Heid, 2011; Shukla and Garg, 2020). Its algorithm works on single-band gray-scale images (Das and Sharma, 2021).

**Table 1.** Description of datasets used for analysis in this study

SL. no.	Dataset	Scene ID	Acquisition date	Spatial resolution (m)	Purpose	Remarks on image quality
1	Declassified data (CORONA)	DS1115-2282DF048	28 Sept 1971	2 m	Terminus delineation	Cloud free, peak ablation period
2	Landsat Enhanced Thematic Mapper	LE07_L1TP_148036_19990716_20200918_02_T1 LE07_L1TP_148036_20021012_20200916_02_T1 LE07_L1TP_148036_20090929_20200911_02_T1	16 Jul 1999 12 Oct 2002 29 Sept 2009	30 m PAN: 15 m	Terminus delineation	Cloud Cover ~2% 8 (%) 7 (%)
3	Sentinel-2A	L1C_T43SET_A032892_20211009T053733	9 Oct 2021	10 m	Terminus mapping	Partial cloud cover, peak ablation
4	Landsat Enhanced Thematic Mapper	LE07_L1TP_148036_19990817_20200918_02_T1 LE07_L1TP_148036_20000904_20200918_02_T1	17 Aug 1999 4 Aug 2000	PAN: 15 m	Surface ice velocity estimation	Cloud <10%
5	Landsat-8 OLI/TIRS	LC08_L1TP_148036_20200903_20200918_02_T1 LC08_L1TP_148036_20210906_20210915_02_T1	18 Aug 2020 15 Aug 2021	PAN: 15 m	Surface ice velocity estimation	Cloud <10%
6	ASTER GDEM	Not applicable	2011	30 m	Topographical information	Not applicable
7.	Field Data (Photographs)	Not applicable	2015 to 2021	Point data	Not applicable	Ground based observations

This study used the panchromatic band of Landsat 8 OLI, 15 m resolution of wavelength 0.50–0.66  $\mu\text{m}$ , and Landsat ETM+ panchromatic (0.52–0.90  $\mu\text{m}$ ) 15 m. The frequency correlation function is employed to get East–West (EW) and North–South (NS) displacements images along with a signal-to-noise ratio (SNR) image. The initial and final window size combination for frequency correlation was set at 64 and 32 pixels, respectively, and the step was set as 2 pixels resulting in a ground resolution of 30 m. The frequency mask threshold and robustness iteration was set as 0.9 and 2, respectively, to reduce the effect of noise on the displacement correlation map. These parameters were chosen based on previous studies on Himalayan glaciers (Gantayat and others, 2014; Sattar and others, 2019; Shukla and Garg, 2020; Das and Sharma, 2021; Kulkarni and others, 2021). Further, post-processing was done to correct potential biases by removing all pixels having SNR <0.9 to discard poorly correlated pixels. After removing erroneous pixels, the resultant displacement was calculated using the Euclidean distance geometry formula.

$$D = \sqrt{x^2 + y^2} \quad (1)$$

Where  $D$  is total displacement,  $x$  is the East–West and  $y$  is North–South displacement.

The acquisition time between the two images ( $t$  days) was then used to compute the ice velocity ( $V$ ) in  $\text{m d}^{-1}$ , which was normalized to annual velocities for 365-day intervals ( $\text{m a}^{-1}$ ).

$$V = (D/t) \times 365 \quad (2)$$

### 3.4. Ice thickness estimation

The ice thickness was estimated by the Himalayan Glacier Thickness Mapper (HIGHTHM) tool (Kulkarni and others, 2019, HIGHTHM manual). The tool was developed based on the laminar flow equation (Eqn 3) and used in recent studies where ice thickness data are unavailable (Gopika and others, 2021; Singh and others, 2023). The glacier boundary, flowlines, moraines, contour polygons in vector format, digital elevation model (DEM) and glacier surface ice velocity in raster format were given as input in the HIGHTHM tool. The glacier thickness, bed topography, and overdeepening sites in the glacier are the output of the HIGHTHM tool. In HIGHTHM, ice thickness is estimated from the laminar flow and basal shear stress equation (8.5) given by Cuffey and Paterson (2010). The laminar flow equation for estimating ice thickness is widely used on the Himalayan glaciers (Gantayat and others, 2014; Maanya and others, 2016;

Remya and others, 2019; Sattar and others, 2019; Gopika and others, 2021).

$$H = \sqrt[4]{\frac{1.5U_s}{Af^3(\rho g \sin \alpha)^3}} \quad (3)$$

Where  $H$  is ice thickness in meters,  $U_s$  is surface ice velocity derived from COSI-Corr,  $\rho$  is the density of ice assigned a constant value of  $900 \text{ kg m}^{-3}$ ,  $g$  is the acceleration due to gravity ( $9.8 \text{ m s}^{-2}$ ),  $A$  is a creep parameter (which depends on temperature, fabric, grain size, and impurity content), assigned a value of  $3.24 \times 10^{-24} \text{ Pa}^{-3} \text{ s}^{-2}$  for temperate glaciers (Cuffey and Paterson, 2010), and  $f$  is shape factor with a constant value 0.8 in the HIGHTHM, i.e. the ratio between the driving stress and basal stress along a glacier (Haeblerli and Hoelzle, 1995),  $\alpha$  is slope estimated from ASTER (GDEM) contours at 100 m intervals.

The ice thickness estimates were obtained by manually digitized flowlines (Linsbauer and others, 2012; Gantayat and others, 2017), and depending upon the size and shape of a glacier, flowlines were interpolated over the entire glacier area to get a  $U$ -shaped glacier thickness distribution, assuming zero ice thickness along the ice margins (Sattar and others, 2019). Therefore, if more than one flowline exists, the flowlines are delineated at a 150 m distance from the glacier margin to 300–400 m from each other to achieve ideal results (Kulkarni and others, 2019; HIGHTHM manual). We draw seven flowlines over the Parkachik Glacier. Further, for the remaining pixels, the spline interpolation technique was used with the boundary condition that ice thickness is maximum along the center flowlines and zero at glacier margins; this gives a complete spatial distribution of glacier depth (Kulkarni and others, 2021).

### 3.5. Uncertainty estimation

The study is based on several multi-satellite data of variable resolution and specifications; therefore, it is liable to introduce errors (Paul and others, 2013). Various errors can be generated from different sources while estimating glacial frontal retreat and other parameters using remote sensing data such as pre-processing, processing, locational/positional, interpretation, and data quality (Racoviteanu and others, 2008, 2009). Therefore, different methods were used to estimate errors induced by the above sources as no common consent between glaciologists is reached for error estimation (Hall and others, 2003; Basnett and others, 2013; Shukla and Qadir, 2016).

Glacier frontal change uncertainty was estimated using the formula given by Hall and others (2003), which was widely used in glacier studies (Shukla and Qadir, 2016; Kumar and others, 2021a)

$$Ut = \sqrt{x_1^2 + x_2^2} + \sigma \quad (4)$$

Where  $Ut$  is terminus uncertainty, ' $x_1$ ' and ' $x_2$ ' are the pixel resolution of images 1 and 2, respectively, and ' $\sigma$ ' is the registration error (Table 2).

Surface ice velocity derived from COSI-Corr-based feature tracking is prone to various errors derived due to orthorectification, substandard image contrast, and poor image correlation (Sahu and Gupta, 2019). Landsat scenes were used for velocity determination, with minimum snow and cloud cover. The cloud-free or <10% cloud cover images were used to minimize the error due to substandard image quality, and ablation zone velocity is considered for glacier dynamics comparative analysis. Image correlation error is minimized by discarding the SNR <0.9.

Velocity error is estimated using the method suggested by (Scherler and others, 2008), and used in other studies (Garg and others, 2022b). Ideally, stable terrain conditions surrounding the glacier should be zero. Velocity error in the stable terrain was calculated based on (Berthier and others, 2003) formula. The CNES/Airbus imagery from Google Earth was used to visually outline the stable terrain. The velocity maps from 1999–2000 and 2020–2021 were utilized as a base map to digitize the stable terrain in the ARC-GIS.

$$\sigma_{\text{off}} = SD_{\text{stable}} + M_{\text{stable}} \quad (5)$$

Where  $\sigma_{\text{off}}$  is the velocity error,  $SD$  is the std dev. in the mean velocity of stable terrain, and  $M_{\text{stable}}$  is the mean velocity of stable terrain. The uncertainty in velocity estimates is calculated for 1999–2000 as  $M_{\text{stable}}$  0.46,  $SD_{\text{stable}}$  1.32, and uncertainty is 1.78, whereas for the year 2020–2021, it is  $M_{\text{stable}}$  0.28,  $SD_{\text{stable}}$  0.52, and uncertainty is 0.80.

Moreover, the uncertainty in glacier thickness estimation depends upon various factors, e.g. surface ice velocity, error in slope determination, shape, and density variation. The combined uncertainty in glacier thickness estimates (based on Eqn. 3) is calculated using the expression below.

$$\frac{dH}{H} = \sqrt{\left(\frac{dU_s}{4U_s}\right)^2 + \left(\frac{3df}{4f}\right)^2 + \left(\frac{3d\rho}{4\rho}\right)^2 + \left(\frac{3dsin\alpha}{4sin\alpha}\right)^2} \quad (6)$$

Where  $dH$  is an error in estimated thickness,  $dU_s$  is the change observed in COSI-Corr-based derived surface ice velocity, glacier shape factor ( $f$ ) ranged between 0.7 in ablation and 0.9 in accumulation zones (Haerberli and Hoelzle, 1995; Linsbauer and others, 2012),  $df$  is uncertainty in shape factor,  $d\rho$  is an error in ice density, and  $dsin\alpha$  is uncertainty due to the DEM. The uncertainty in surface ice velocity comes due to orthorectification error, misregistration between the images, and limitations of the

COSI-Corr correlation technique (Maanya and others, 2016; Sattar and others, 2019). Co-registration accuracy of 5 m for Landsat imagery is taken from Gopika and others (2021), and COSI-Corr accuracy for correlation is in the order of  $\sim 1/20$ th of a pixel or 1.5 m (Leprince and others, 2007).

No field-based velocity data for the glaciers from this region are available to validate the velocity estimates. The estimated mean velocity of  $0.80 \text{ m a}^{-1}$  on the stable ground by the COSI-Corr method is considered an error. The combined velocity error is calculated as  $5 \text{ m a}^{-1}$ . Considering the typical variation in ice density from 830 to 923 ( $\text{kg m}^{-3}$ ),  $\pm 10\%$  uncertainty in ice density is considered, as suggested by Bhambri and others (2015) and Remya and others (2019). The shape factor varies with  $\pm 0.1$ , giving a relative uncertainty of (12.5%) (Gantayat and others, 2014; Maanya and others, 2016). The uncertainty in slope estimation arises from DEM vertical inaccuracy. Fujita and others (2008) reported an 11 m vertical inaccuracy for ASTER DEM in the Bhutan Himalayan region. Due to the topographical similarity, similar vertical inaccuracy is considered, and  $\pm 9\%$  uncertainty for the  $\sin\alpha$  value is estimated. A combined uncertainty of  $\pm 14.68\%$  was calculated. Further, the uncertainty of  $\pm 6.5\%$  in ice thickness arises due to the interpolation algorithm taken from Hutchinson (2011). Therefore, the overall HIGTHIM tool estimated ice thickness uncertainty is  $\pm 16\%$ .

## 4. Results

### 4.1. Frontal retreat and morphological changes

The glacier has a sudden change in slope (approximately 1.5 km upstream from the glacier terminus) in the lower ( $\sim 16^\circ$ ) and upper ablation zone ( $9^\circ$ ). Due to the variability in slope, the glacier retreat is oscillatory.

Overall the glacier retreated by  $-210 \pm 88 \text{ m}$  with an average rate of  $4 \pm 1 \text{ m a}^{-1}$  between 1971 and 2021. The snout of the Parkachik Glacier indicates different fluctuation patterns in various sectors (Fig. 2). Based on the satellite data, the glacier retreat is calculated in 1971–1999 and 1999–2021. The overall retreat of the glacier between 1971 and 1999 was  $-54 \pm 18 \text{ m}$  with an average rate of  $2 \pm 0.6 \text{ m a}^{-1}$ . Whereas, between 1999 and 2021, the glacier retreated  $-246 \pm 62 \text{ m}$  with an average rate of  $12 \pm 3 \text{ m a}^{-1}$ . Moreover, an advance of the snout of approximately  $44 \pm 29 \text{ m}$  with an average rate of  $15 \pm 10 \text{ m a}^{-1}$  was observed between 1999 and 2002. This may result from subglacial cavity collapse resulting in a lateral spread of ice and disintegration of the marginal zone. It has also been observed that the glacier snout broke down and blocked the glacier stream for an unknown duration and formed a temporary lake beneath the glacier in 2017 (Fig. 3a). After a few hours, that lake breached, and the broken ice blocks spread around the proglacial area (Fig. 3b). This was observed in the field (2017) discharge data (Fig. 3c), when the emerging stream from the glacier suddenly disappeared for an hour followed by an outburst flood scattering about ice blocks up to  $\sim 200 \text{ m}$  downstream of the ice margin.

Similarly, the field observations from 2015 to 2021 show that the glacier retreated by  $-123 \pm 72 \text{ m}$  at an average rate of  $-20.5 \pm 12 \text{ m a}^{-1}$ . The left part of the glacier showed a higher retreat of  $-254 \pm 150 \text{ m}$ , whereas the right part was quasi-stagnant and retreated only  $-26 \pm 13 \text{ m}$  between 2015 and 2021. After 2015 it was observed (in the field) that the glacier front is continuously breaking, and ice-collapsing events are happening regularly. This increased the disintegration and frontal lowering of the glacier between 2015 and 2021. Moreover, the glacier surface (from terminus to upper ablation zone) between 3650 and 3800 m a.s.l. was covered with supraglacial debris of variable thickness ( $< 1 \text{ cm}$  to  $> 1 \text{ m}$ ) and with sediment sizes varying from silts and sand to

**Table 2.** Uncertainty in terminus position change estimated as per Hall and others (2003), using Eqn 4

Satellite sensor	Terminus change uncertainty (m)
CORONA (1971)-ETM+ (1999)	18
ETM+ (1999)-(2002)	23
ETM+ (2002)-(2009)	25
ETM+ (2009)-Sentinel-2A (2021)	20
CORONA (1971)-Sentinel-2A (2021)	19

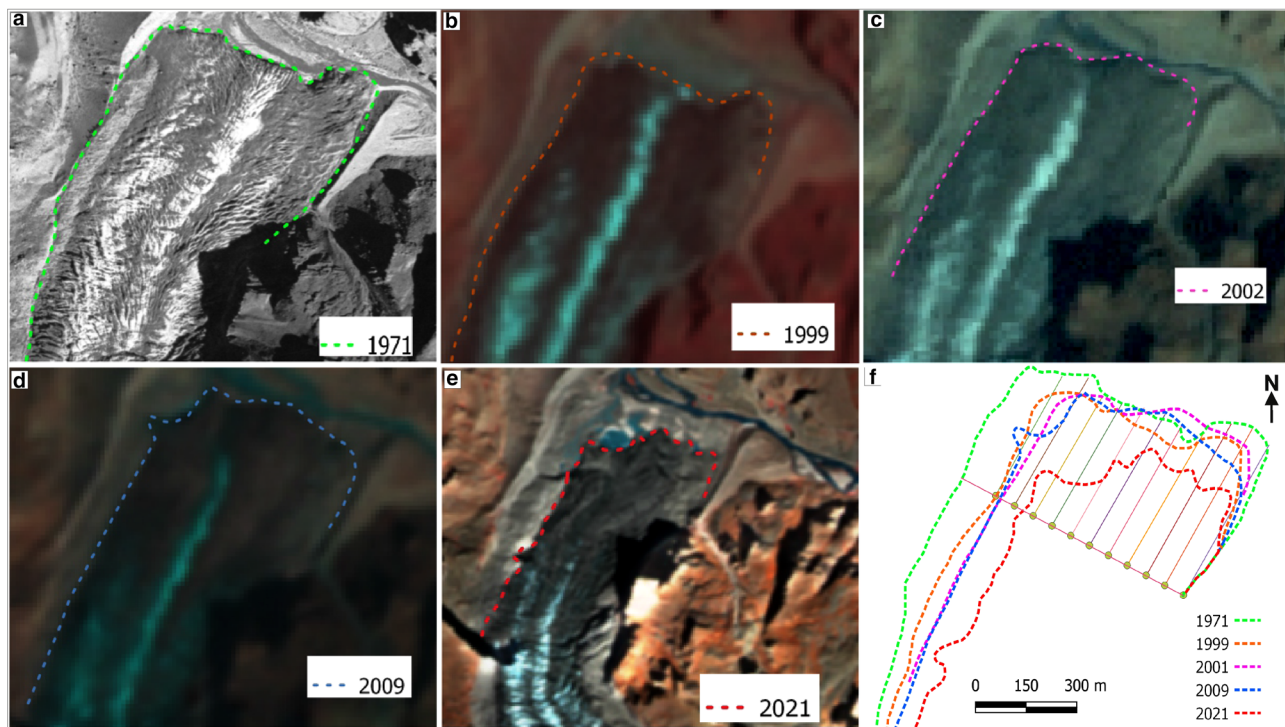


**Figure 2.** Satellite images of different years showing the glacier margin. (a) CORONA KH-4 image, 1971, (b) Landsat ETM+, 1999, (c) Landsat ETM+, 2002, (d) Landsat ETM+, 2009, (e) Sentinel-2A, 2021. (f) Overall margin fluctuations from 1971 to 2021.

large boulders exceeding several meters. This variable debris thickness also plays a critical role in glacier melting (Dobhal and others, 2013; Mehta and others, 2021, 2023). The details about the glacier retreat and morphological changes are given in Table 3 and Fig. 4.

#### 4.2. Frontal area loss

The frontal area loss was calculated over the same time intervals (1971–2021) as the recession was calculated, and within this period, the rates were variable but accelerated after the year 2009

(Table 4). Further, field evidence revealed that an ice cave was formed at the left portion of the glacier snout (present in 2015) that collapsed (in 2018) could be a probable reason for the enhanced retreat and area loss of the left flank (Fig. 5).

#### 4.3. Surface ice velocity

The surface ice velocity of the Parkachik Glacier was computed for the years 1999–2000 and 2020–2021. The overall trend of decreasing glacier velocity was found in 2020–2021 compared to 1999–2000. Only ablation zone velocity estimates were considered for comparative study due to poor image contrast in the accumulation zone, leading to erroneous velocities due to data voids. The velocity over the lower ablation zone during 1999–2000 was estimated to be  $45.18 \pm 1.78 \text{ m a}^{-1}$  which was reduced to  $32.28 \pm 0.80 \text{ m a}^{-1}$  between 2020 and 2021. The velocity trends were observed based on three flowlines drawn on the left, central, and right parts of the glacier ablation zone (Fig. 6). The results show a similar overall trend in all flowlines (Fig. 7). Further, the recent velocity of 2020–2021 was correlated with NASA ITS\_LIVE velocity extracted from (<https://its-live.jpl.nasa.gov/>). The present study velocity estimates show a positive correlation ( $R: 0.80$ ) with the

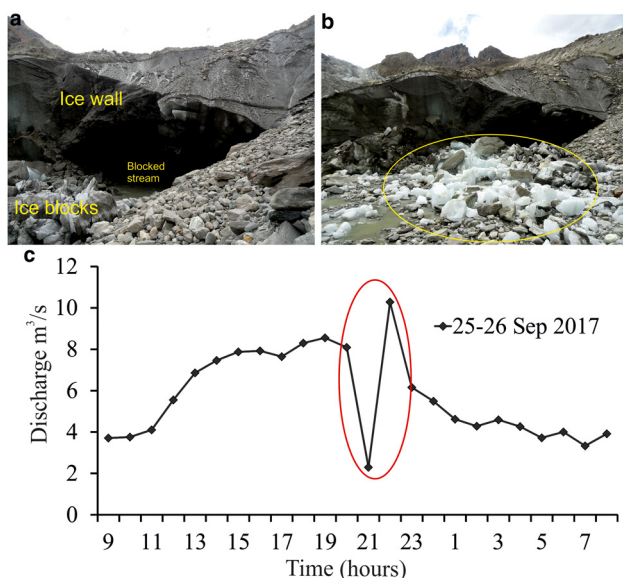


**Figure 3.** (a) and (b) are the field photographs showing the blocked stream and broken ice blocks after the outburst flood. (c) Field discharge data showing suddenly low and high peaks (red circle) in a discharge after the block and release of energy (Fig. c is modified after Garg and others, 2018). The spread ice blocks are clearly shown in Figure b.

**Table 3.** Frontal retreat of the glacier calculated using satellite data and field observations over the past five decades

Year	Total retreat (–)/Advance (+) (m)			Average total retreat (m)	Retreat rate ( $\text{m a}^{-1}$ )
	Right part	Central part	Left part		
<b>I- Satellite data</b>					
1971–1999	$-55 \pm 27$	$-54 \pm 7$	$-54 \pm 20$	$-54 \pm 18$	$-2 \pm 0.6$
1999–2002	$+43 \pm 33$	$+77 \pm 38$	$+14 \pm 16$	$+45 \pm 3$	$+15 \pm 1$
2002–2009	$-52 \pm 23$	$-22 \pm 12$	$-15 \pm 11$	$-30 \pm 15$	$-4 \pm 2$
2009–2021	$-116 \pm 23$	$-127 \pm 38$	$-270 \pm 17$	$-171 \pm 26$	$-14 \pm 2$
Total retreat	$-180 \pm 106$	$-126 \pm 95$	$-325 \pm 64$	$-210 \pm 88$	$-4 \pm 1$
<b>II- In-situ measurement</b>					
2015–2018	$-5 \pm 3$	$-50 \pm 25$	$-109 \pm 70$	$-54 \pm 32$	$-18 \pm 11$
2018–2021	$-21 \pm 10$	$-40 \pm 25$	$-145 \pm 80$	$-69 \pm 38$	$-23 \pm 13$
Total retreat	$-26 \pm 13$	$-90 \pm 50$	$-254 \pm 150$	$-123 \pm 70$	$-20 \pm 12$

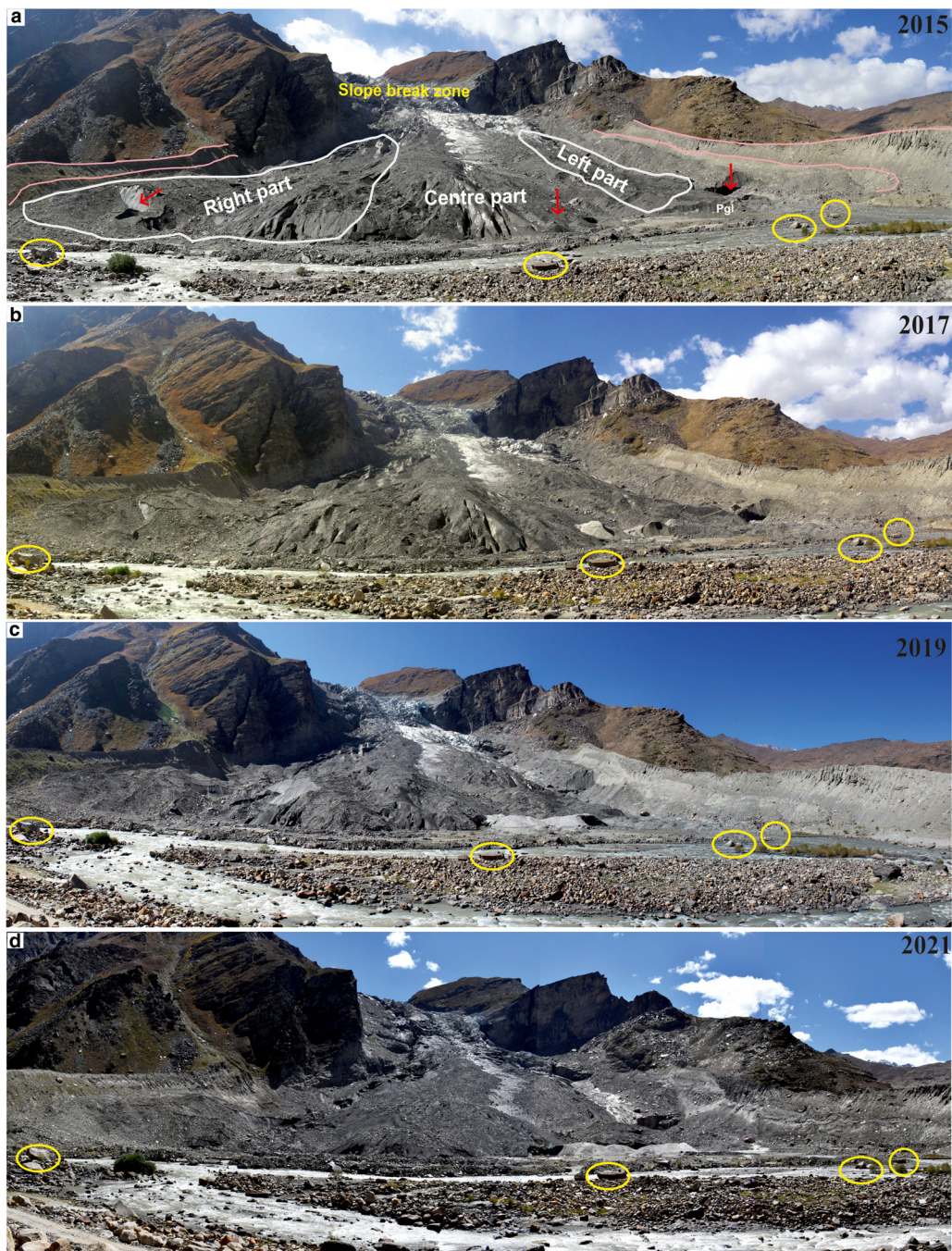


**Figure 4.** Field photographs (a to d) from 2015, 2017, 2019, and 2021 (two years intervals), showing the panoramic view of the glacier front and lower ablation zone that was divided into three parts, i.e. left, centre, and right (shown in photo a). (a) Is also showing slope break zone, lateral moraines (light pink color lines), red arrows indicating the changes observed between 2015 and 2021, and yellow circles highlighting the ground control points (stable boulders) taken as reference points for frontal (retreat) monitoring. (a) Showing the location of the proglacial (pgl) lake formed at the left of the glacier terminus.

ITS\_LIVE velocity (Fig. 8). However, we have considered only those velocities for comparative analysis which were derived from Landsat 8 images having the temporal resolution of 345–370 days between image-pairs.

An anomalous behavior (advancement) of the glacier between 1999 and 2002 can be understood with abnormal velocity change at the terminus. The glacier terminus showed high velocity from 1999 to 2000 compared to other parts of the glacier, whereas in the slope break zone (3950 m a.s.l.) sudden drop in velocity is seen compared to 2020–2021. The terminus region may be influenced by a proglacial lake or subglacial drainage that might collapse in 1999–2000, increasing the terminus velocity. This suggests that the glacial advancement of 1999–2002 is related to the abnormal velocity in the lower (at terminus) and upper ablation (slope break) zones.

**Table 4.** Frontal area loss by the glacier between 1971 and 2021

Period	Frontal area loss (km <sup>2</sup> )	Frontal area gain (km <sup>2</sup> )	Net area change (km <sup>2</sup> )
1971–1999	0.098	Nil	−0.098
1999–2002	0.015	0.027	+0.012
2002–2009	0.024	0.007	−0.017
2009–2021	0.125	Nil	−0.125

#### 4.4. Ice thickness and overdeepenings

The average ice thickness of the Parkachik Glacier was estimated to be  $115 \pm 16$  m. The thickness of the glacier varies from the terminus to the accumulation zone. Figure 9 clearly



**Figure 5.** (a) And (b) Field photos (2015 and 2018) show both calving, collapse, and general thinning of the glacier front. The orange boxes show an ice cave present in 2015 and collapsed in 2018. The yellow circle in both photos shows the reference boulders (~4 m in length) for change detection.

shows the variability in ice thickness as it is lower (~44 to 83 m) at the terminus, between 200 and 350 m in the upper ablation zone, and reaches ~441 m in the accumulation zone; however, these estimates need to be verified by ground-based measurements. Here, we have compared the present study thickness estimates with the global dataset of Farinotti and others (2019). The present study estimated the average ice thickness of  $115 \pm 18$  m with a maximum thickness of 441 m, whereas Farinotti and others (2019) average thickness was 135 m showing a maximum of 382 m. Such differences arise as thickness estimates were derived from different models and

input datasets, including the glacier outline. The most significant differences in glacier thickness are found along the glacier boundaries, where the present study shows lower thickness estimates than Farinotti and others (2019), and in the deepest parts of the glacier (Fig. 10).

We have identified three potential overdeepening sites for lake formation on the glacier at different elevations (from lower to upper ablation zone) with a mean depth of 34 to 84 m. However, the expansion and reduction of these lakes depend on the dynamics of the glacier. The estimated future lake depth, area, and water volume are given in Table 5 and Fig. 11.

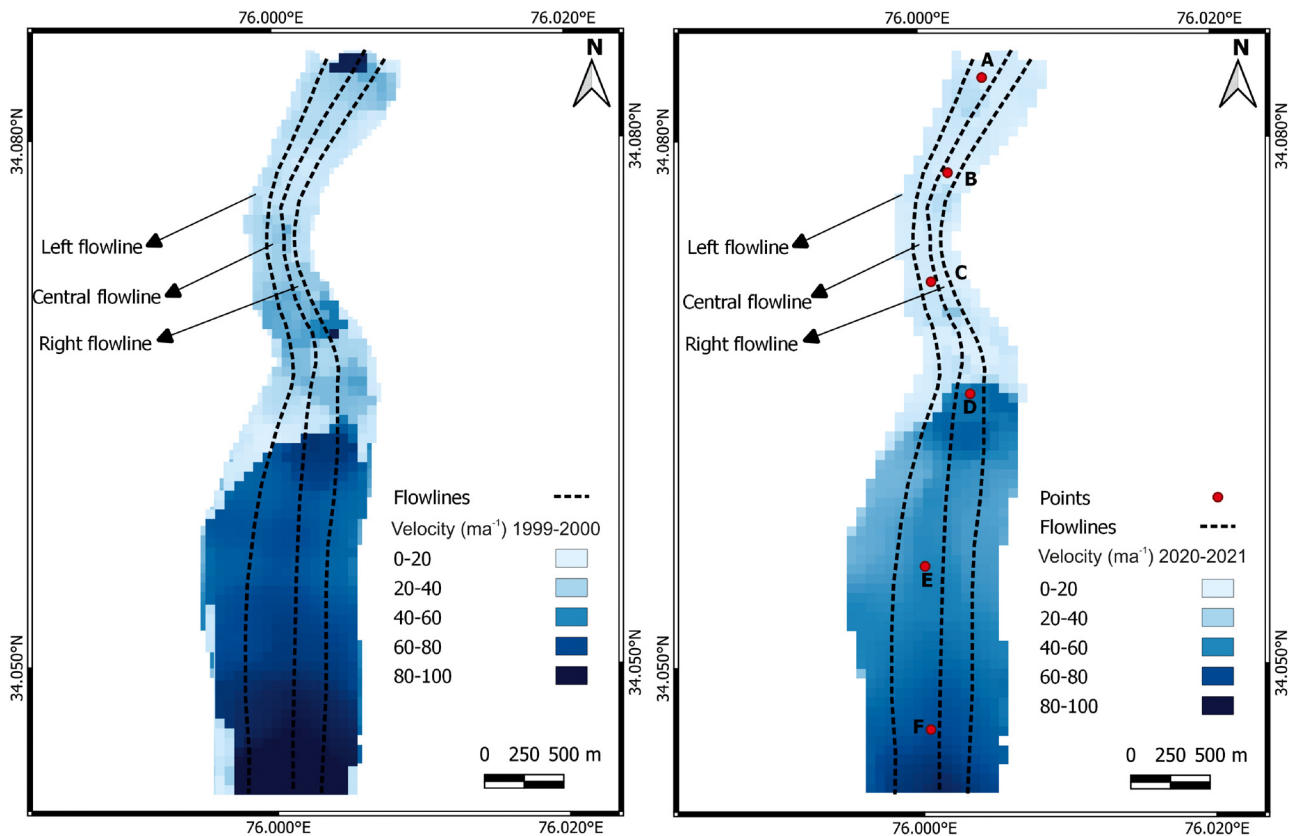


**Figure 6.** Surface ice velocity for 1999–2000 and 2020–2021. The red dots are the points taken to compare the present study velocity estimates with the ITS\_LIVE velocity.

## 5. Discussion

The glaciers in the Suru River valley are generally characterized by their geographical position covering two major ranges, i.e. the Great Himalayan Range and Ladakh Range, at high altitudes, their large size, and the dominance of partially debris-covered ice. The recent glacier inventory of the Suru Basin has suggested a heterogeneity in glacier response (Shukla and others, 2020a, 2020b). Shukla and others (2020a) reported the overall average retreat rate of the glaciers was  $4.3 \pm 1.02 \text{ m a}^{-1}$  between 1971 and 2017. Kamp and others (2011) suggested a retreat of  $\sim 13 \text{ m a}^{-1}$  and a re-advancement of  $17 \text{ m a}^{-1}$  for the years 1979–1990 and 1990–1999 of the Parkachik Glacier. Rai and others (2013) reported a retreat of 1300 m with an average of  $33 \text{ m a}^{-1}$  between 1962 and 2001 of the glaciers in the Doda Basin, Zaskar and Jammu & Kashmir region. Schmidt and Nüsser (2017) reported a retreat of 248 m with an average of  $5.3 \text{ m a}^{-1}$  between 1969 and 2002 in the Central Ladakh Range. Similarly, the overall frontal recession ( $4 \pm 1 \text{ m a}^{-1}$  between 1971 and 2021) of the glacier reported in this study is consistent with the other studies across the northwest Himalaya (Murtaza and Romshoo, 2017; Shukla and others, 2017; Mir and Majeed, 2018; Rashid and Majeed, 2018; Shukla and Garg, 2019; Mehta and others, 2021). However, the recent retreat rate ( $-20 \pm 12 \text{ m a}^{-1}$ , since 2015) derived from the field survey is higher than other regional studies (Bahuguna and others, 2014; Ghosh and others, 2014; Rashid and Majeed, 2018). The accelerated glacier retreat after 2015 in this study suggests the influence of the proglacial lake and the disintegration of the marginal zone of the Parkachik Glacier. Mir and Majeed (2018) suggested that the Parkachik Glacier retreated 127 m at a rate of  $2.9 \text{ m a}^{-1}$  between 1971 and 2015, which is underestimated, whereas Garg and others (2022b) overestimated the glacier recession and reported an

overall recession of  $497 \pm 32 \text{ m}$  with an average retreat of  $11 \pm 0.7 \text{ m a}^{-1}$  between 1971 and 2018. This discrepancy in a recession may largely be ascribed due to the difference in the time frame, resolution of data, field observations (GCPs) and validation, and methodology used for inferring the changes.

Further, the surface ice velocity estimation in this study suggests a slowing down which is primarily due to down wasting and deglaciation, resulting in an increase of debris cover on the glacier surface (ablation zone) and an insufficient supply of snow in the accumulation zone over the past two decades (Garg and others, 2017; Shukla and Garg, 2019; Garg and others, 2022a, 2020b). However, the higher velocity transfer more mass down the glacier, compensating for the glacier recession (Tiwari and others, 2014; Shukla and Garg, 2019).

Maanya and others (2016) estimated the ice thickness of the Durung-Drung Glacier, one of the largest glaciers in Doda Basin, Zaskar ( $\sim 63 \text{ km}$  from the Parkachik Glacier) derived from the laminar flow equation (Eqn 3) as 100 m at the terminus and 50–400 m in the accumulation zone. Moreover, they identified three potential lake sites with mean depths varying between 40 and 75 m. Similarly, a recent study carried out on Durung-Drung Glacier reported the ice thickness of the glacier between 1 and 311 m with a mean thickness of 155 using the GlabTop (Glacier-bed Topography) model (Rashid and Majeed, 2018). In addition, Rashid and Majeed (2018) speculated the formation of 76 potential lakes with varying depths between 7 and 222 m, which is more than the estimates of Maanya and others (2016). In this study, the maximum thickness was estimated to be  $\sim 441 \text{ m}$  in the upper reaches, 350–440 at the center, and 44–80 m at the terminus of the Parkachik Glacier. Rashid and Majeed (2018) suggested that the Durung-Drung could be a suitable glacier for extracting an ice core because of its location in a

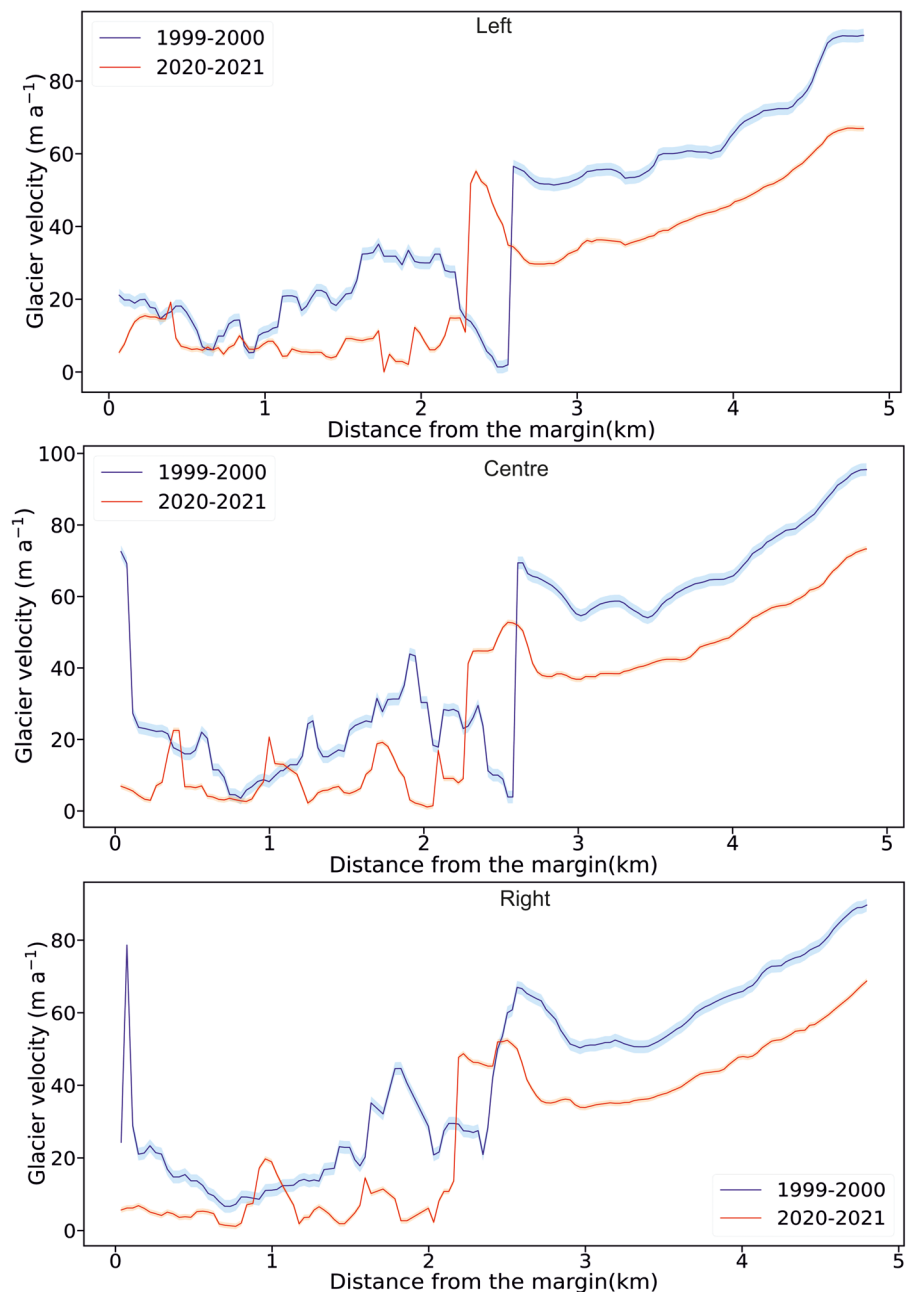


Figure 7. Surface ice velocity of the glacier left, central, and right parts in 1999–2000 and 2020–2021.

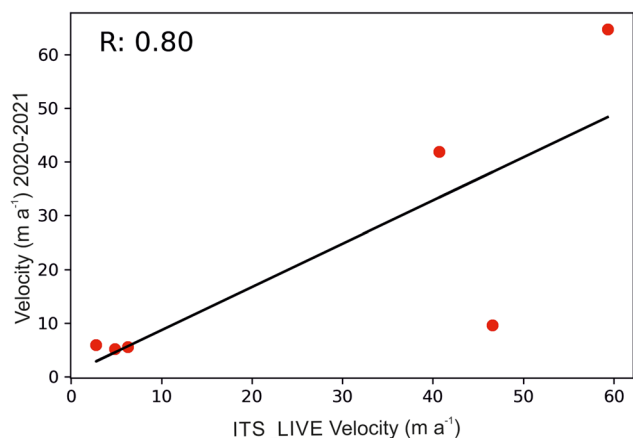


Figure 8. Present study velocity estimates show a positive correlation ( $R: 0.80$ ) compared to the ITS\_LIVE velocity.

cold arid climate with an ice thickness of  $>300$  m in the accumulation zone. Similarly, after estimating the thickness of the Parkachik Glacier, we can speculate that the glacier can be a better site for ice core drilling as its estimated maximum depth (441 m) is more than the Durung-Drung Glacier. Although the thickness and overdeepenings site data from this region is very scarce, comparing the present study estimates with the recent studies (Maanya and others, 2016; Rashid and Majeed, 2018) suggests that this study is consistent with other studies in the region and provides credible information about the ice thickness and probability of development of glacial lakes at different sites.

### 6. Conclusion

In this study, we analyzed multiple glacier parameters (frontal area, glacier thickness, surface ice velocity, bed overdeepenings, and morphological changes) for the Parkachik Glacier, western Himalaya.

We have estimated the ice thickness for Parkachik Glacier from surface velocities and slopes using the laminar flow equation

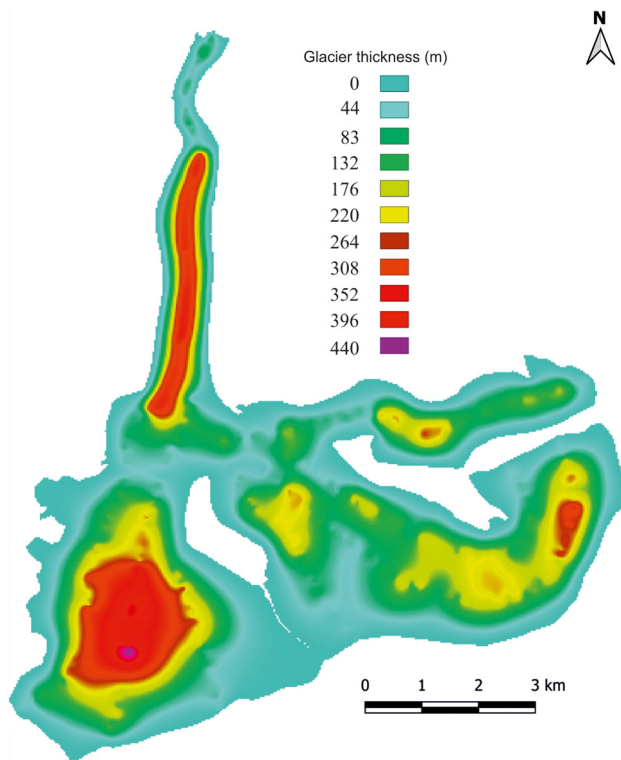


**Figure 9.** Modelled (a) ice thickness of the glacier varying from ~44 to 83 m near the terminus, between 200 and 350 m in the upper ablation zone, and reaching >400 m in the accumulation zone. Maximum thickness is modelled as 440 m.

(Eqn 3). The surface velocity slowed down from 45 to 32 m a<sup>-1</sup> over the past two decades (1999–2021). The ice thickness attained a maximum value of 441 m in the upper reaches, a range of 350–440 m was found in the middle, and the lower reaches, the range was 44–80 m. Further, using surface ice velocity and slopes, along with basal shear stress and the laminar flow equation, glacier thickness and bed topography were estimated. We identified three potential overdeepening sites for lake formation on the glacier at different elevations (from lower to upper ablation zone) with a mean depth of 34 to 84 m.

**Table 5.** Calculated overdeepenings for future lake development with lake area, mean depth, and water volume

Lake ID	Lake area (ha)	Mean depth (m)	Maximum depth (m)	Water volume (million m <sup>3</sup> )
A	159.54	84.34	223.25	134 ± 25
B	43.29	34.92	106.90	14 ± 3
C	271.30	48.04	121.23	129 ± 24

Overall the glacier retreat varied between 1971 and 2021. The glacier retreated with an average rate of 2 ± 0.6 m a<sup>-1</sup> between 1971 and 1999. Whereas between 1999 and 2021, the glacier retreated at an average rate of 12 ± 3 m a<sup>-1</sup>. Similarly, the field observations suggest that the glacier retreated at a higher rate of -20.5 ± 12 m a<sup>-1</sup> between 2015 and 2021. The field and satellite-based observations indicate that the calving nature of the glacier margin and the development of a proglacial lake may have enhanced the retreat of the Parckachik Glacier. The significant slowdown, extensive surface lowering, progressive growth and expansion of the proglacial lake at the terminus, and consecutive calving of the snout since 2015 suggest accelerated glacier demise.

The comparison of the modelled ice thickness in this study with the other studies (Farinotti and others, 2017; Sattar and others, 2019) shows that the method is well suited to estimate the ice thickness of the glacier in the region. The Ice Thickness Models Intercomparison eXperiment (ITMIX1) concluded the comparison between various models, as the most reasonable ice thickness estimate can be derived by averaging multiple models. In contrast, the analyses conducted in ITMIX2 do not reveal a singularly superior model among the various models evaluated. However, the Tasman Glacier (valley glacier) Gantayat model was highly reliable and efficient. Also, the small model bias in the Gantayat model is comparable to other thickness models that revealed its performance (Farinotti and others, 2017; Sattar and others, 2019). Whereas the HIGTHIM used in this study was considered a simple tool in which the selected inputs are required. Therefore, because of its simplicity and less input, the Gantayat model, based on which the HIGTHIM tool produces a reliable output in ITMIX. While other mass conservation approaches require glacier mass balance data, some shear stress-based models also require mass balance data for thickness and

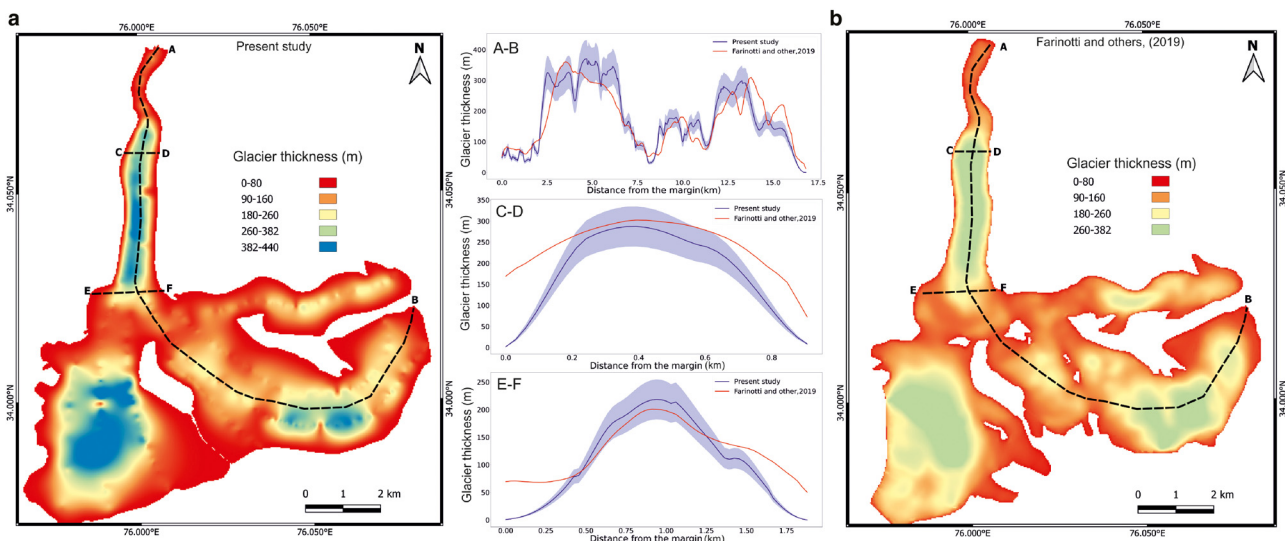


**Figure 10.** Comparison of the present study thickness estimates with the freely available dataset of Farinotti and others (2019). Ice thickness was compared for the three sections (A–B, C–D, and DE). Significant changes in glacier thickness are found along the glacier margin, where the present study shows fewer thickness estimates than Farinotti and others (2019).

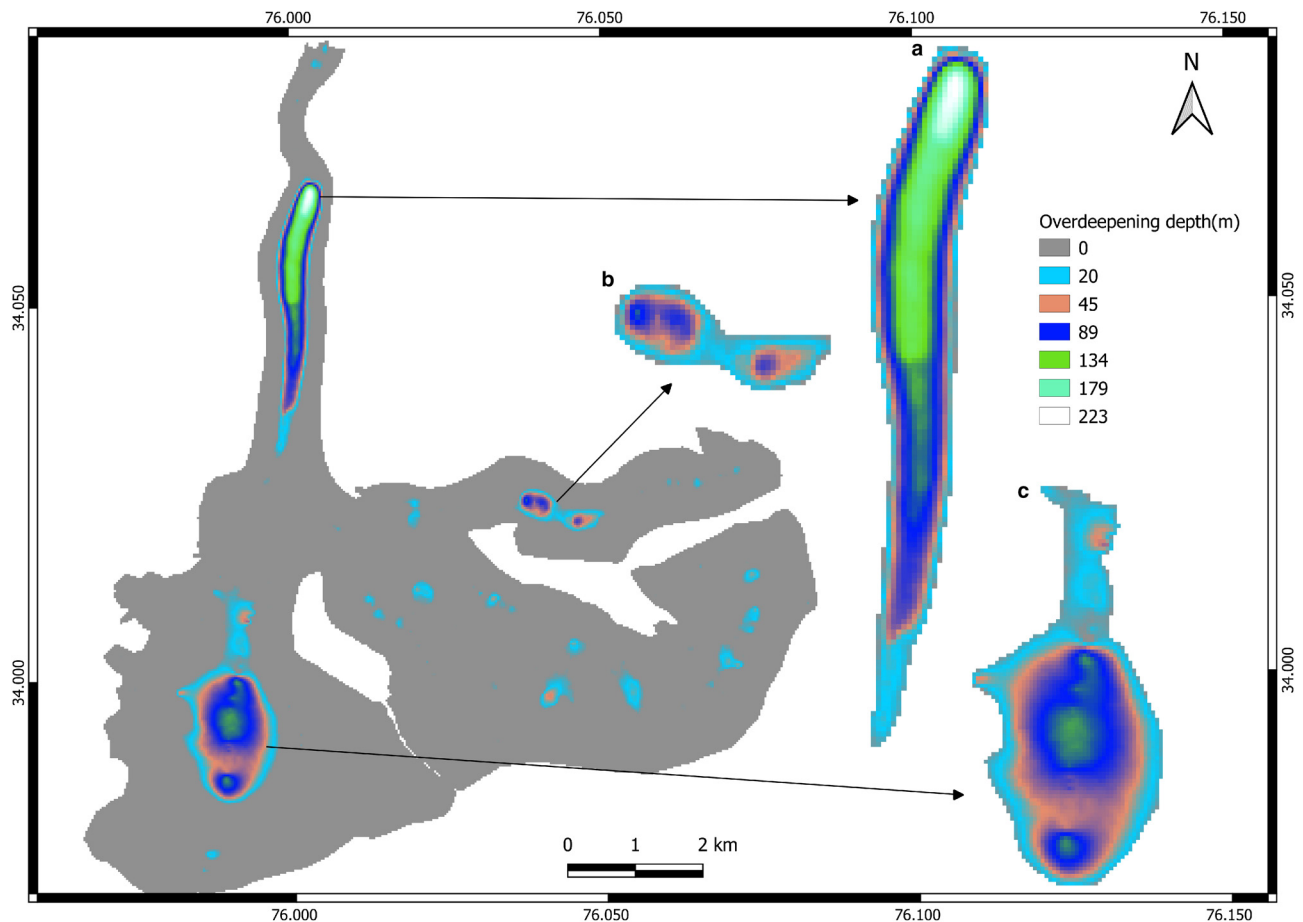


**Figure 11.** Overdeepenings under the glacier with predicted lake sites (a, b, and c) with depths varying from 20 to 223 m.

volume estimates. However, due to the sparse mass balance and limited ground-based ice thickness measurements from the study area, the approach adopted in this study can be assumed reliable for ice thickness estimation in future studies.

**Acknowledgments.** The authors are grateful to the Director of Wadia Institute of Himalayan Geology (WIHG), Dehra Dun, India, for providing the necessary facilities and support to carry out this work. We are also thankful to the Department of Science and Technology, Ministry of Science and Technology, Government of India, for financial support to carry out this work. The authors thank Dr. Aparna Shukla (Scientist, Ministry of Earth Sciences, New Delhi) and the local people of Parkachik and Rangdum villages, Ladakh, for their assistance during the field campaign. The authors wish to convey their sincere thanks to Prof. Hester Jiskoot -Chief Editor IGS and anonymous reviewers for their detailed reviews, beneficial suggestions, and constructive comments, which immensely helped and improved the manuscript previous version. This is WIHG contribution number WIHG/0239.

**Data availability statement.** The data presented in this paper are available upon request from the corresponding author.

## References

- Akhtar M, Ahmad N and Booij MJ (2008) The impact of climate change on the water resources of Hindukush–Karakorum–Himalaya region under different glacier coverage scenarios. *Journal of Hydrology* **355**(1–4), 148–163.
- Azam MF and 10 others (2016) Meteorological conditions, seasonal and annual mass balances of Chhota Shigri Glacier, western Himalaya, India. *Annals of Glaciology* **57**(71), 328–338. doi: [10.3189/2016AoG71A570](https://doi.org/10.3189/2016AoG71A570)
- Bahuguna IM and 6 others (2014) Are the Himalayan glaciers retreating? *Current Science* **106**(7), 1008–1013.
- Basnett S, Kulkarni AV and Bolch T (2013) The influence of debris cover and glacial lakes on the recession of glaciers in Sikkim Himalaya, India. *Journal of Glaciology* **59**(218), 1035–1046. doi: [10.3189/2013JoG12J184](https://doi.org/10.3189/2013JoG12J184)
- Berthier E, Raup B and Scambos T (2003) New velocity map and mass-balance estimate of Mertz glacier, East Antarctica, derived from Landsat sequential imagery. *Journal of Glaciology* **49**(167), 503–511.
- Bhambri R, Bolch T and Chaujar RK (2012) Frontal recession of Gangotri Glacier, Garhwal Himalayas, from 1965 to 2006, measured through high-resolution remote sensing data. *Current Science* **102**(3), 489–494.
- Bhambri R, Mehta M, Dobhal, DP and Gupta AK (2015) *Glacier Lake Inventory of Uttarakhand*. Dehradun, India: Wadia Institute of Himalayan Geology.
- Bhushan S, Syed TH, Arendt AA, Kulkarni AV and Sinha D (2018) Assessing controls on mass budget and surface velocity variations of glaciers in Western Himalaya. *Science Report* **8**, 8885. doi: [10.1038/s41598-018-27014-y](https://doi.org/10.1038/s41598-018-27014-y)
- Bolch T and 6 others (2012) The state and fate of Himalayan glaciers. *Science* **336**(6079), 310–314.
- Brun F, Berthier E, Wagnon P, Käab A and Treichler D (2017) A spatially resolved estimate of High Mountain Asia glacier mass balances from 2000 to 2016. *Nature Geoscience* **10**(9), 668–673.
- Chand P and Sharma M C (2015) Glacier changes in the Ravi basin, North-Western Himalaya (India) during the last four decades (1971–2010/13). *Global and Planetary Change* **135**, 133–147.
- Cuffey KM and Paterson WSB (2010) *The Physics of Glaciers*. Burlington, MA: Butterworth-Heinemann, Elsevier.
- Das S and Sharma MC (2021) Glacier surface velocities in the Jankar Chhu watershed, western Himalaya, India: study using Landsat time series data (1992–2020). *Remote Sensing Applications: Society and Environment* **24**, 1–23.
- Dobhal DP, Mehta M and Srivastava D (2013) Influence of debris cover on terminus retreat and mass changes of Chorabari Glacier, Garhwal region, central Himalaya, India. *Journal of Glaciology* **59**(217), 961–971.
- Dobhal DP, Pratap B, Bhambri R and Mehta M (2021) Mass balance and morphological changes of Dokriani Glacier (1992–2013), Garhwal Himalaya, India. *Quaternary Science Advances* **4**, 1–9.
- Farinotti D and 23 others (2017) How accurate are estimates of glacier ice thickness? Results from ITMIX, the ice thickness models intercomparison eXperiment. *The Cryosphere* **11**(2), 949–970.

- Farinotti D and 6 others** (2019) A consensus estimate for the ice thickness distribution of all glaciers on Earth. *Nature Geoscience* **12**(3), 168–173.
- Frey H and 9 others** (2014) Estimating the volume of glaciers in the Himalayan–Karakoram region using different methods. *The Cryosphere* **8** (6), 2313–2333. doi: [10.5194/tc-8-2313-2014](https://doi.org/10.5194/tc-8-2313-2014)
- Fujita K, Suzuki R, Nuimura T and Sakai A** (2008) Performance of ASTER and SRTM DEMs, and their potential for assessing glacial lakes in the Lunana region, Bhutan Himalaya. *Journal of Glaciology* **54**(185), 220–228.
- Gantayat P, Kulkarni AV and Srinivasan J** (2014) Estimation of ice thickness using surface velocities and slope: case study at Gangotri Glacier, India. *Journal of Glaciology* **60**(220), 277–282. doi: [org/10.3189/2014JG013J078](https://doi.org/10.3189/2014JG013J078)
- Gantayat P, Kulkarni AV, Srinivasan J and Schmeits MJ** (2017) Numerical modelling of past retreat and future evolution of Chhota Shigri glacier in Western Indian Himalaya. *Annals of Glaciology* **58**(75), 136–144. doi: [10.1017/aog.2017.21](https://doi.org/10.1017/aog.2017.21)
- Garg S and 6 others** (2018) Field evidence showing rapid frontal degeneration of the Kangriz glacier, western Himalayas, Jammu & Kashmir. *Journal of Mountain Science* **15**(6), 1199–1208.
- Garg PK and 5 others** (2022a) Stagnation of the Pensilungpa glacier, western Himalaya, India: causes and implications. *Journal of Glaciology* **68**(268), 221–235. doi: [10.1017/jog.2021.84](https://doi.org/10.1017/jog.2021.84)
- Garg S, Shukla A, Garg PK, Yousuf B and Shukla UK** (2022b) Surface evolution and dynamics of the Kangriz glacier, western Himalaya in past 50 years. *Cold Regions Science and Technology* **196**, 1–15.
- Garg S, Shukla A, Mehta M, Kumar V and Shukla UK** (2019) On geomorphic manifestations and glaciation history of the Kangriz glacier, western Himalaya. *Himalayan Geology* **40**(2), 115–127.
- Garg PK, Shukla A, Tiwari RK and Jasrotia AS** (2017) Assessing the status of glaciers in part of the Chandra basin, Himachal Himalaya: a multiparametric approach. *Geomorphology* **284**, 99–114.
- Ghosh S, Pandey AC, Nathawat MS and Bahuguna IM** (2014) Contrasting signals of glacier changes in Zaskar valley, Jammu & Kashmir, India using remote sensing and GIS. *Journal of the Indian Society of Remote Sensing* **42**(4), 817–827.
- GlaThiDa Consortium** (2019) *Glacier Thickness Database 3.0.1*. Zurich, Switzerland: World Glacier Monitoring Service. doi: [10.5904/wgms-glathida-2019-03](https://doi.org/10.5904/wgms-glathida-2019-03)
- Goossens R, De Wulf A, Gheyle W and Bourgeois J** (2006) Estimation of the permafrost area in the Altai Mountains (Russia) in the framework of the preservation of the frozen tombs of the Altai Mountains. In *Global Developments in Environmental Earth Observation from Space: Proceedings of the 25th Symposium of the European Association for Remote Sensing Laboratories*, 595–601.
- Gopika JS, Kulkarni AV, Prasad V, Srinivasalu P and Raman A** (2021) Estimation of glacier stored water in the Bhaga basin using laminar flow and volume-area scaling methods. *Remote Sensing Applications: Society and Environment* **24**(100656), 2352–9385. doi: [10.1016/j.rsase.2021.100656](https://doi.org/10.1016/j.rsase.2021.100656)
- Haeblerli W and Hoelzle M** (1995) Application of inventory data for estimating characteristics of and regional climate-change effects on mountain glaciers: a pilot study with the European Alps. *Annals of Glaciology* **21**, 206–212.
- Hall DK, Bayr KJ, Schöner W, Bindschadler RA and Chiene JYL** (2003) Consideration of the errors inherent in mapping historical glacier positions in Austria from the ground and space (1893–2001). *Remote Sensing of Environment* **86**, 566–577. doi: [10.1016/S0034-4257\(03\)00134-2](https://doi.org/10.1016/S0034-4257(03)00134-2)
- Harris I, Osborn TJ, Jones P and Lister D** (2020) Version 4 of the CRU TS monthly high-resolution gridded multivariate climate dataset. *Science Data* **7**, 109. <https://doi.org/10.1038/s41597-020-0453-3>.
- Heid T** (2011) *Deriving glacier surface velocities from repeat optical images* (Ph.D. Thesis). Department of Geosciences, Faculty of Mathematics and Natural Sciences, University of Oslo, Norway.
- Hutchinson MF** (2011) *ANUDEM Version 5.3, User Guide*. Canberra: Fenner School of Environment and Society, Australian National University.
- Kamp U, Byrne M and Bolch T** (2011) Glacier fluctuations between 1975 and 2008 in the Greater Himalaya Range of Zaskar, Southern Ladakh. *Journal of Mountain Science* **8**, 374–389. doi: [10.1007/s11629-011-2007-9](https://doi.org/10.1007/s11629-011-2007-9)
- Kaushik S, Joshi PK and Singh T** (2019) Development of glacier mapping in Indian Himalaya: a review of approaches. *International Journal of Remote Sensing* **40**(17), 6607–6634.
- Kayastha R B and Harrison S P** (2008) Changes of the equilibrium-line altitude since the Little Ice Age in the Nepalese Himalaya. *Annals of Glaciology* **48**, 93–99.
- King O, Bhattacharya A, Bhambri R and Bolch T** (2019) Glacial lakes exacerbate Himalayan glacier mass loss. *Scientific Reports* **9**(1), 1–9.
- Kulkarni A and 9 others** (2019) HIMALAYAN GLACIER THICKNESS MAPPER (HIGTHIM) USER MANUAL. Number of pages 34. This tool is written in Python and gives spatial distribution of glaciers, bottom topography and location and extent of potential glacier lake. To get the tool, contact [glacier.dccc@iisc.ac.in](mailto:glacier.dccc@iisc.ac.in).
- Kulkarni A, Prasad V and Shirsat T** (2021) Impact of climate change on the glaciers of Spiti river basin, Himachal Pradesh, India. *Journal Indian Soc Remote Sensing* **49**, 1951–1963. doi: [10.1007/s12524-021-01368-9](https://doi.org/10.1007/s12524-021-01368-9)
- Kumar V and 5 others** (2021b) Glacier changes and associated climate drivers for the last three decades, Nanda Devi region, Central Himalaya, India. *Quaternary International* **575**, 213–226.
- Kumar V, Mehta M, Mishra A and Trivedi A** (2017) Temporal fluctuations and frontal area change of Bangni and Dunagiri glaciers from 1962 to 2013, Dhauliganga Basin, central Himalaya, India. *Geomorphology* **284**, 88–98.
- Kumar V, Mehta M and Shukla T** (2021a) Spatially resolved estimates of glacial retreat and lake changes from Gepang Gath Glacier, Chandra Basin, Western Himalaya, India. *Journal of the Geological Society of India* **97**(5), 520–526.
- Kumar V, Mehta M, Shukla A, Kumar A and Garg S** (2021c) Late Quaternary glacial advances and equilibrium-line altitude changes in a semi-arid region, Suru Basin, western Himalaya. *Quaternary Science Reviews* **267**, 1–22.
- Kumari S and 5 others** (2021) Modelling ice thickness distribution and volume of Patsio Glacier in Western Himalayas. *Journal of Earth System Science* **130**(3), 1–14.
- Lee E and 5 others** (2021) Accelerated mass loss of Himalayan glaciers since the Little Ice Age. *Scientific reports* **11**(1), 1–8.
- Leprince S, Ayoub F, Klingler Y and Avouac JP** (2007) Co-registration of optically sensed images and correlation (COSI-Corr): An operational methodology for ground deformation measurements. *IEEE international geoscience and remote sensing symposium*, 1943–1946.
- Linsbauer A, Paul F and Haeblerli W** (2012) Modeling glacier thickness distribution and bed topography over entire mountain ranges with GlabTop: application of a fast and robust approach. *Journal of Geophysical Research: Earth Surface* **117**, 1–17.
- Maanya US, Kulkarni AV, Tiwari A, Bhar ED and Srinivasan J** (2016) Identification of potential glacial lake sites and mapping maximum extent of existing glacier lakes in Drang Drung and Samudra Tapu glaciers, Indian Himalaya. *Current Science* **111**(3), 553–560.
- Mal S, Mehta M, Singh RB, Schickhoff U and Bisht MPS** (2019) Recession and morphological changes of the debris-covered Milam Glacier in Gori Ganga Valley Central Himalaya India derived from satellite data. *Frontiers in Environmental Science* **7**(42), 1–17. doi: [10.3389/fenvs.2019.00042](https://doi.org/10.3389/fenvs.2019.00042)
- Mehta M, Kumar V, Garg S and Shukla A** (2021) Little Ice Age glacier extent and temporal changes in annual mass balance (2016–2019) of Pensilungpa Glacier, Zaskar Himalaya. *Regional Environmental Change* **21**(38), 1–18. doi: [10.1007/s10113-021-01766](https://doi.org/10.1007/s10113-021-01766)
- Mehta M, Kumar V, Kunmar P and Sain K** (2023) Response of the thick and thin debris-covered glaciers between 1971 and 2019 in Ladakh Himalaya, India – a case study from Pensilungpa and Durung-Drung glaciers. *Sustainability* **15**(5), 1–21.
- Millan R, Mouginot J, Rabatel A and Morlighem M** (2022) Ice velocity and thickness of the world's glaciers. *Nature Geoscience* **15**(2), 124–129.
- Mir RA and Majeed Z** (2018) Frontal recession of Parkachik Glacier between 1971–2015, Zaskar Himalaya using remote sensing and field data. *Geocarto International* **33**(2), 163–177.
- Mishra A, Nainwal HC, Dobhal DP and Shankar R** (2021) Volume estimation of glaciers in Upper Alaknada Basin, Garhwal Himalaya using numerical and scaling methods with limited field-based data. *Himalayan Geology* **42**(2), 336–344.
- Mishra A, Nainwal HC and Shankar R** (2022) Glacier ice thickness estimation in Indian Himalaya using geophysical methods: a brief review. In Pandey M, Pandey PC, Ray Y, Arora A, Jawak SD and Shukla UK (eds), *Advances in Remote Sensing Technology and the Three Poles*, First Edition. Hoboken, NJ: John Wiley & Sons Ltd., pp. 299–307.
- Mishra A, Negi BDS, Banerjee A, Nainwal HC and Shankar R** (2018) Estimation of ice thickness of the Satopanth Glacier, Central Himalaya using ground penetrating radar. *Current Science* **114**(4), 785–791.

- Murtaza KO and Romshoo SA** (2017) Recent glacier changes in the Kashmir alpine Himalayas, India. *Geocarto International* **32**(2), 188–205.
- Nie Y and 6 others** (2021) Glacial change and hydrological implications in the Himalaya and Karakoram. *Nature Reviews Earth & Environment* **2**(2), 91–106.
- Nüsser M and Schmidt S** (2021) Glacier changes on the Nanga Parbat 1856–2020: a multi-source retrospective analysis. *Science of the Total Environment* **785**, 1–12.
- Paul F and 19 others** (2013) On the accuracy of glacier outlines derived from remote-sensing data. *Annals of Glaciology* **54**(63), 171–182.
- Pieczonka T, Bolch T, Kröhnert M, Peters J and Liu S** (2018) Glacier branch lines and glacier ice thickness estimation for debris-covered glaciers in the Central Tien Shan. *Journal of Glaciology* **64**(247), 835–849.
- Pratap B, Dobhal DP, Bhambri R, Mehta M and Tewari VC** (2016) Four decades of glacier mass balance observations in the Indian Himalaya. *Regional Environmental Change* **16**, 643–658.
- Pratap B, Dobhal DP, Mehta M and Bhambri R** (2015) Influence of debris cover and altitude on glacier surface melting: a case study on Dokriani Glacier, central Himalaya, India. *Annals of Glaciology* **56**(70), 9–16.
- Racoviteanu AE, Arnaud Y, Williams MW and Ordoñez J** (2008) Decadal changes in glacier parameters in the Cordillera Blanca, Peru, derived from remote sensing. *Journal of Glaciology* **54**(186), 499–510. doi: [10.3189/002214308785836922](https://doi.org/10.3189/002214308785836922)
- Racoviteanu AE, Paul F, Raup B, Khalsa SJS and Armstrong R** (2009) Challenges and recommendations in mapping of glacier parameters from space: results of the 2008 Global Land Ice Measurements from Space (GLIMS) Workshop, Boulder, Colorado, USA. *Annals of Glaciology* **50**(53), 53–69. doi: [10.3189/172756410790595804](https://doi.org/10.3189/172756410790595804)
- Rai PK, Nathawat MS and Mohan K** (2013) Glacier retreat in Doda Valley, Zaskar Basin, Jammu & Kashmir, India. *Universal Journal of Geoscience* **1**, 139–149.
- Rashid I and Majeed U** (2018) Recent recession and potential future lake formation on Drang Drung glacier, Zaskar Himalaya, as assessed with earth observation data and glacier modelling. *Environmental Earth Sciences* **77**(12), 1–13.
- Remya SN, Kulkarni AV, Pradeep S and Shrestha DG** (2019) Volume estimation of existing and potential glacier lakes, Sikkim Himalaya, India. *Current Science* **116**(4), 620–627.
- Sahu R and Gupta RD** (2019) Surface velocity dynamics of Samudra Tapu Glacier, India from 2013 to 2017 using Landsat-8 data. *ISPRS Annals of the Photogrammetry, Remote Sensing and Spatial Information Sciences* **4**, 75–81.
- Sattar A, Goswami A, Kulkarni AV and Das P** (2019) Glacier-surface velocity derived ice volume and retreat assessment in the Dhauliganga basin, central Himalaya: a remote sensing and modeling-based approach. *Frontiers in Earth Science* **7**(105), 1–15.
- Scherler D, Leprince S and Strecker MR** (2008) Glacier-surface velocities in alpine terrain from optical satellite imagery—Accuracy improvement and quality assessment. *Remote Sensing Environment* **112**(10), 3806–3819.
- Schmidt S and Nüsser M** (2009) Fluctuations of Raikot Glacier during the past 70 years: a case study from the Nanga Parbat massif, northern Pakistan. *Journal of Glaciology* **55**, 949–959.
- Schmidt S and Nüsser M** (2017) Changes of high-altitude glaciers in the Trans-Himalaya of Ladakh over the past five decades (1969–2016). *Geosciences* **7**(2), 1–15.
- Schmidt S, Nüsser M, Baghel R and Dame J** (2020) Cryosphere hazards in Ladakh: the 2014 Gya glacial lake outburst flood and its implications for risk assessment. *Natural Hazards* **104**, 2071–2095.
- Shugar DH and 6 others** (2020) Rapid worldwide growth of glacial lakes since 1990. *Nature Climate Change* **10**(10), 939–945.
- Shukla A and Ali I** (2016) A hierarchical knowledge-based classification for glacier terrain mapping: a case study from Kolahoi Glacier, Kashmir Himalaya. *Annals of Glaciology* **57**(71), 1–10.
- Shukla A, Ali I, Hasan N and Romshoo SA** (2017) Dimensional changes in the Kolahoi glacier from 1857 to 2014. *Environmental Monitoring and Assessment* **189**(1), 1–18.
- Shukla A and Garg PK** (2019) Evolution of a debris-covered glacier in the western Himalaya during the last four decades (1971–2016): a multiparametric assessment using remote sensing and field observations. *Geomorphology* **341**, 1–14. doi: [10.1016/j.geomorph.2019.05.009](https://doi.org/10.1016/j.geomorph.2019.05.009)
- Shukla A and Garg PK** (2020) Spatio-temporal trends in the surface ice velocities of the central Himalayan glaciers, India. *Global and Planetary Change* **190**, 1–16.
- Shukla A, Garg S, Kumar V, Mehta M and Shukla UK** (2020b) Sensitivity of glaciers in part of the Suru river valley, Western Himalaya to ongoing climatic perturbations. In Dimri AP, Bookhagen B, Stoffel M and Yasunari T (eds), *Himalayan Weather and Climate and Their Impact on the Environment*. New York: Springer International Publishing, pp. 351–377.
- Shukla A, Garg S, Mehta M, Kumar V and Shukla UK** (2020a) Temporal inventory of glaciers in the Suru sub-basin, western Himalaya: impacts of the regional climate variability. *Earth System Science Data* **12**, 1245–1265.
- Shukla A, Garg PK and Srivastava S** (2018) Evolution of glacial and high-altitude lakes in the Sikkim, Eastern Himalaya over the past four decades (1975–2017). *Frontiers in Environmental Science* **6**(81), 1–19.
- Shukla A and Qadir J** (2016) Differential response of glaciers with varying debris cover extent: evidence from changing glacier parameters. *International Journal of Remote Sensing* **37**(11), 2453–2479.
- Shukla T and Sen IS** (2021) Preparing for floods on the Third Pole. *Science* **372**(6539), 232–234.
- Singh H and 6 others** (2023) Assessment of potential present and future glacial lake outburst flood hazard in the Hunza valley: a case study of Shispar and Mochowar glacier. *Science of the Total Environment* **868**, 1–18.
- Tiwari RK, Gupta RP and Arora MK** (2014) Estimation of surface ice velocity of Chhota-Shigri glacier using sub-pixel ASTER image correlation. *Current Science* **106**(6), 853–859.
- Welty E and 12 others** (2020) Worldwide version-controlled database of glacier thickness observations. *Earth System Science Data* **12**(4), 3039–3055.
- Workman FB and Workman WH** (1909) *Peaks and Glaciers of Nun Kun: A Record of Pioneer-Exploration and Mountaineering in the Punjab Himalaya*. London: Royal Geographical Society.
- Zemp M and 6 others** (2019) Global glacier mass changes and their contributions to sea-level rise from 1961 to 2016. *Nature* **568**(7752), 382–386.